

## ELECTRONIC SUPPLEMENTARY INFORMATION

### Synergistic Switching of Plasmonic Resonances and Molecular Spin States

Khaldoun Abdul-Kader,<sup>a</sup> Manuel Lopes,<sup>a</sup> Carlos Bartual-Murgui,<sup>b</sup> Olena Kraieva,<sup>a,c</sup> Edna M. Hernández,<sup>a</sup> Lionel Salmon,<sup>a</sup> William Nicolazzi,<sup>a</sup> Franck Carcenac,<sup>b</sup> Christophe Thibault,<sup>b</sup> Gábor Molnár<sup>\*a</sup> and Azzedine Bousseksou<sup>\*a</sup>

<sup>a</sup>LCC, CNRS and Université de Toulouse (UPS, INP), Toulouse, France, E-mail : [boussek@lcc-toulouse.fr](mailto:boussek@lcc-toulouse.fr); [molnar@lcc-toulouse.fr](mailto:molnar@lcc-toulouse.fr)

<sup>b</sup>LAAS, CNRS and Université de Toulouse (UPS, INSA, ISAE), Toulouse, France

<sup>c</sup>Kyiv Polytechnic Institute, National Technical University of Ukraine, Kyiv, Ukraine

### EXPERIMENTAL DETAILS

*Elaboration of the LSP substrate.* First a 140 nm thick polymethylmetacrylate (PMMA) resist was spin coated on the surface of a glass substrate and baked at 170 °C for 2 min. Due to the insulating nature of the substrate a 20 nm thick Ge layer was deposited on top of the resist by thermal evaporation. The PMMA was then nano-patterned using a RAITH150 e-beam writer operating at 20 kV. 20 arrays were patterned, on each substrate, with geometries ranging from 50 nm <  $L$  < 300 nm,  $W = 50$  or 100 nm, and  $G_x, G_y = 100$  or 200 nm. Then the Ge layer was removed by an H<sub>2</sub>O<sub>2</sub> (30 %) solution and the exposed resist was developed in a 1:3 mixture of methyl isobutyl ketone (MIBK) and isopropyl alcohol (IPA). The sample was soaked in pure IPA to stop the developing process and dried in a nitrogen flow. After development, the substrate was covered successively by 5 nm Ti and 45 nm Au, deposited by thermal evaporation. Finally, lift-off was achieved by immersing the wafer in acetone for 15 min at room temperature, followed by 5 min agitation in an ultrasonic bath of absolute ethanol.

*Deposition of the spin transition layer on the LSP substrate.* The preparation of a homogeneous chloroform solution of the SCO complex [Fe(hptrz)<sub>3</sub>](OTs)<sub>2</sub> was previously discussed.<sup>27</sup> Thin films of the complex were prepared by spin coating the chloroform solution

on the LSP substrates. The film thickness was adjusted by changing the spinning velocity and the concentration of the complex.

*Sample characterization.* AFM images were acquired using a Dimension Icon (Bruker) microscope equipped with an OTESPA tip. Scans were performed in air at room temperature in tapping mode. SEM images were recorded with a Hitachi S-4800 microscope operating at 1 kV. For the variable-temperature LSPR measurements the samples were enclosed in a THMS-600 liquid-nitrogen cryostat (Linkam Scientific Instruments). Before the LSPR experiments the samples were dehydrated at 90 °C under N<sub>2</sub> flow for ~20 min and were kept under N<sub>2</sub> atmosphere during the spectrum acquisitions - unless otherwise stated. The micro-spectrometer used for collecting LSPR spectra in the 400-1100 nm range consists of a BX51 (Olympus) optical microscope, which was fiber coupled to a Shamrock 303i (Andor Technology) spectrograph equipped with a 150 mm<sup>-1</sup> grating and a DU420-BV charge-coupled device detector (see also [fig. S7](#)). The entrance slit was kept at 200 μm to match the diameter of the fiber. The nanorod array was illuminated by linearly polarized white light (polarization axis parallel to the nanorod axis) using a halogen lamp and an Abbe condenser, whose aperture was closed down to its minimum (numerical aperture,  $NA = 0.1$ ). The transmitted light was collected using a ×10 magnification objective ( $NA = 0.25$ ). The spectra recorded on the gold nanorod arrays (delimited by the field diaphragm of the microscope) were first divided by a reference spectrum (recorded through the glass substrate) and then fitted to a Gaussian lineshape to extract the value of  $\lambda_{LSPR}$ . During the photo-thermal experiments the gold nanorod arrays were excited by the 633 nm radiation of a 3 mW HeNe laser, which was directed through appropriate neutral density filters and was focused on the sample via the microscope objective. The laser polarization direction was fixed parallel to the axis of the nanorods. A narrow stop-band filter (centered at 633 nm) was used to prevent the laser radiation to reach the spectrograph.

**Figure S1.** (a) AFM topography image of a gold nanorod array. (b) The corresponding height distribution histogram indicates *ca.* 50 nm thickness for the metallic layers (Ti + Au) deposited on the glass substrate.

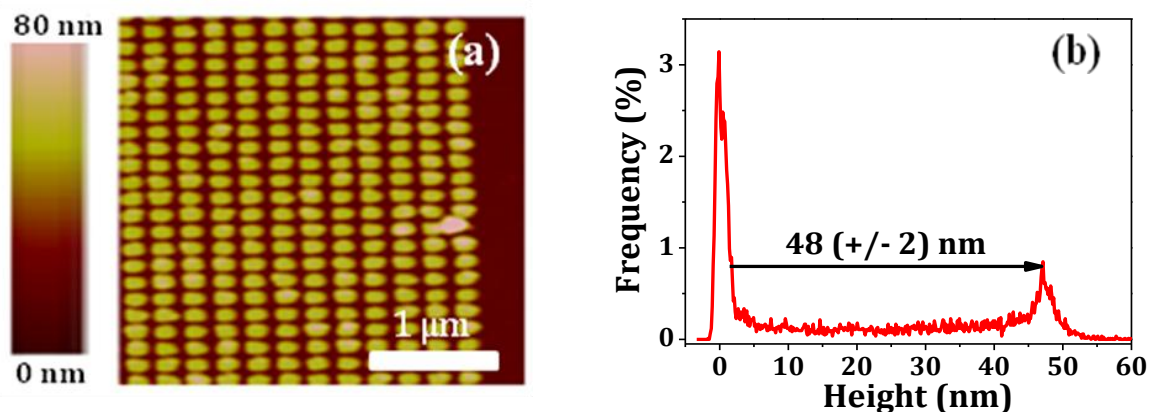


**Figure S2.** (a) Extinction spectra of gold nanorod arrays for different lengths (100, 150, 200, 250, 300 nm), with 100 nm width and 50 nm height. (b) Variation of the extinction peak wavelength as a function of the nanorod length. The solid line is a linear fit on the experimental data ( $\lambda_{LSPR} = 486 (\pm 10) + 1.37 (\pm 0.05) \times L$ ). All data were collected in ambient air.

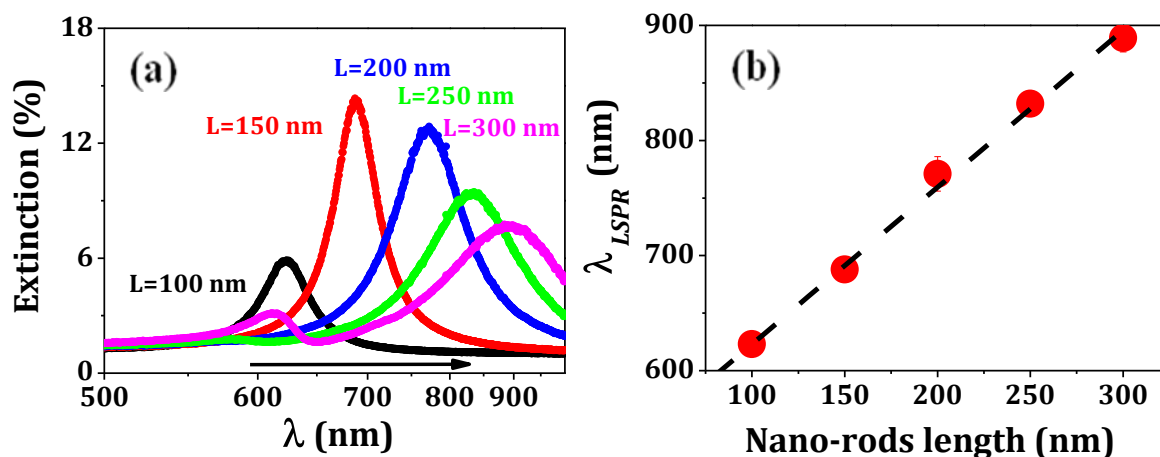


**Figure S3.** Relationship between the refractive index and the LSPR peak maximum for the three gold nanorod arrays shown in figure 1. Dry nitrogen ( $n = 1$ ), water ( $n = 1.33$ ) and a microscopy oil ( $n = 1.52$ ) were used for the measurements ( $T = 293$  K). The straight lines are linear fits, which gave the following values of  $S$ :  $217 \pm (4)$  nm/RIU (array **1c**),  $160 \pm (8)$  nm/RIU (array **1b**) and  $125 \pm (2)$  nm/RIU (array **1a**), respectively. (These data were used to construct fig. 1f.)

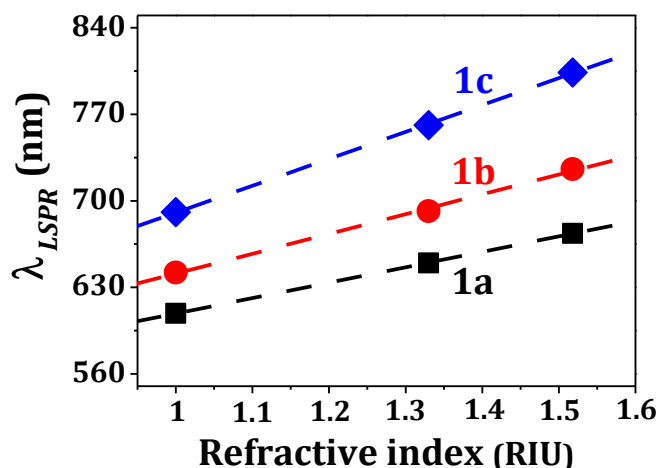


**Figure S4.** Left panel: AFM topographical images of thin films with different thickness of the complex  $[\text{Fe}(\text{hptrz})_3](\text{OTs})_2$  deposited on the LSP substrate. Right panel: Height distribution histograms extracted from the corresponding AFM images for the film thickness measurement. (These data were used to construct [fig. 3](#).)

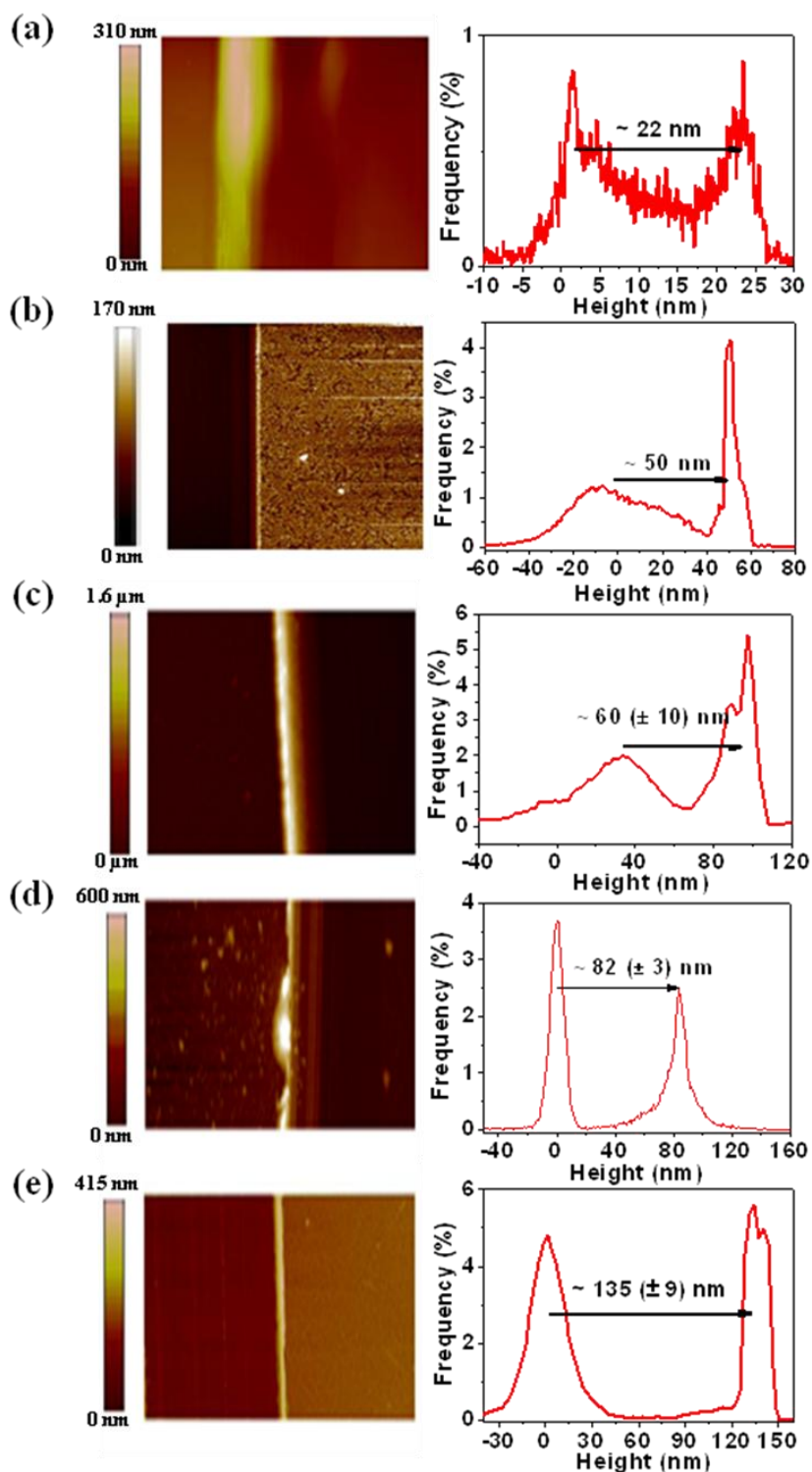


**Figure S5.** (a) Extinction spectrum for different thin film thickness ( $d = 22, 50, 60, 82$  and  $135$  nm) of the SCO complex  $[\text{Fe}(\text{hptrz})_3](\text{OTs})_2$  deposited on the gold nanorod array with an initial  $\lambda_{\text{LSPR}}$  value of  $718$  nm. (These data were used to construct fig. 3.) (b) Extinction spectra before (thick lines) and after (thin lines) the deposition of a  $60$  nm thick film of  $[\text{Fe}(\text{hptrz})_3](\text{OTs})_2$  on different gold nanorod arrays ( $L = 100, 150, 200$  and  $250$  nm). (c) LSPR peak wavelength following the film deposition as a function of the initial LSPR wavelength. The blue squares correspond to different film thickness, while the red circles correspond to the same film thickness ( $60$  nm) on different arrays. All data were collected in ambient air. The red line is a linear fit on the red circles. The diagonal black dashed line is inserted only to guide the eye. The lack of parallelism between the two lines reflects the increasing LSPR sensitivity ( $S$ ) with increasing LSPR wavelength.

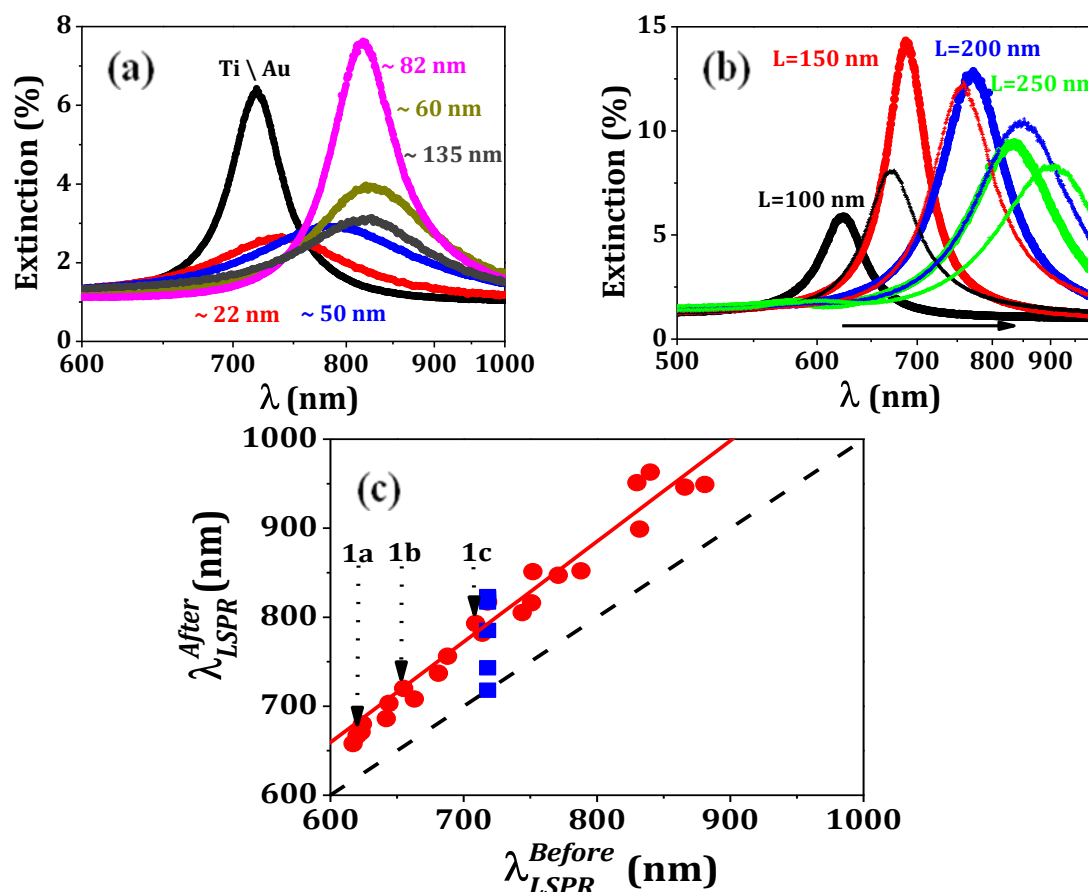


**Figure S6.** (a) Spectral overlap of the  $633$  nm pump laser line with the plasmon resonances of the nanorod arrays used in the photo-thermal experiments displayed in fig. 5. (b) Variation of the LSPR wavelength as a function of the pump laser intensity for a  $[\text{Fe}(\text{hptrz})_3](\text{OTs})_2$  coated ( $60$  nm) gold nanorod array. Filled (empty) symbols indicate increasing (decreasing) laser power.

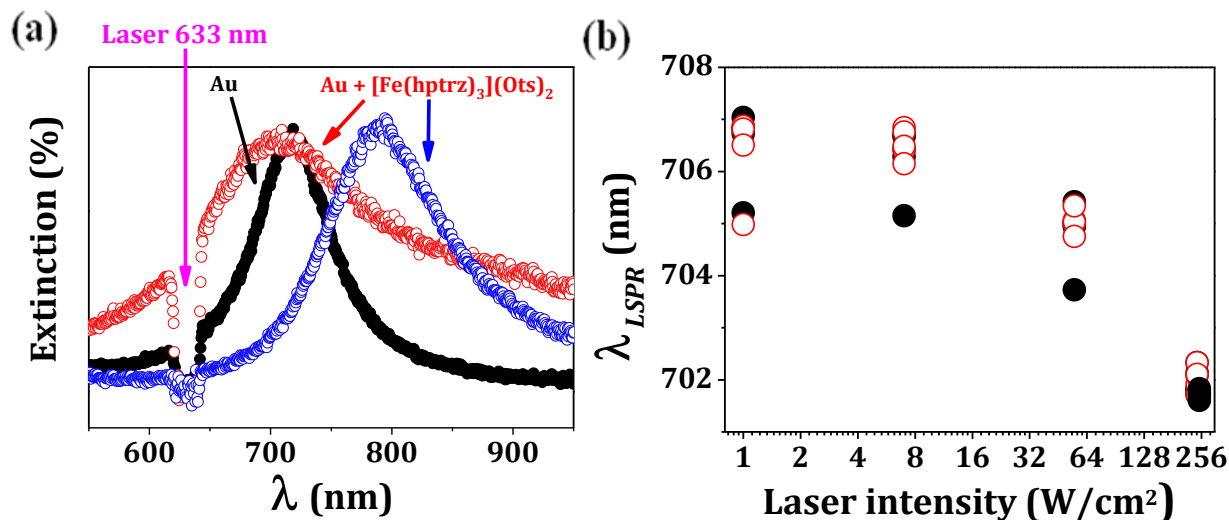


**Figure S7.** Scheme of the optical microscopy (Olympus BX51) setup used for extinction spectra measurements.

